VOL. 6, NO. 6, JUNE 2011 ISSN 1819-6608
ARPN Journal of Engineering and Applied Sciences

www.arpnjournals.com

MECHANICS OF DEFORMATION DURING OPEN DIE FORGING OF SINTERED PREFORM: COMPARATIVE STUDY BY EQUILIBRIUM AND UPPER BOUND METHODS

Parveen Kumar[1], R. K. Ranjan[2] and Rajive Kumar[3]
[1]Department of Mathematics, BRCM, CET, Bahal (Bhiwani), India
[2]Department of Mechanical Engineering, Gyan Ganga Institute of Technology and Sciences, Jabalpur, India
[3]Department of Mathematics, DCR University of Science and Technology, Murthal (Sonepat), India
E-Mail: parveen_brcm@rediffmail.com

ABSTRACT

The paper reports on an investigation into the various aspects of open die forging of metal powder preforms, which have been compacted and sintered from atomized metal powder. An attempt has been made for the determination of the relative average die pressure developed for given geometries of the disc during the open die forging of sintered metal powder preform by using an upper bound and equilibrium method approach as different frictional stresses are assumed on top and bottom interfaces. The deformation characteristics of metal powder preform has been demonstrated by applying an appropriate interfacial friction law and yield criteria. The results so obtained are discussed critically to illustrate the interaction of various process parameters involved and are presented graphically.

Keywords: open die forging, sintered preform, interfacial friction law, upper bound and equilibrium method.

INTRODUCTION

Metal powder technology is currently arousing interests in many parts of the world as producing components from metal powders are much economical. Sinter forming is a rapidly developing near net shape mass production technology, in which compacted metal powder preforms are formed within the dies to produce precise, high performance and economically competitive engineering components. The final density of such sinter formed products compares favorably with that of wrought products [1, 2]. The technology has extensive applications in the field of automobiles, aerospace, defense and other household products, e.g. connecting rods, rears, crankshafts, engine, etc. [3-5].

This paper concerns the pressure distribution at the work piece interface and die load during the cold forging of the disc at low speed, during the analysis an appropriate interfacial friction law and yield criterion for porous metal is used. The sinter forming technology is entirely different from conventional wrought metal forming, as characteristics of porous materials during compression have to be taken into consideration. The densification (compaction or closing of pores) and compression (change of shape) of sintered preform takes place simultaneously during sinter forming process and hence volumetric constancy principle is not valid, as density of preform changes due to closing of inter particle pores. Thus, the sensitivity of yielding on hydrostatic stress component necessitates the use of suitable yield criterion, which is dependent on relative density of preform [6, 7]. The high interfacial pressure applied for deformation breaks the die-work piece interfacial lubricant film and creates the conditions; are modeled as composite friction including both sliding and sticking friction [8, 9].

Recently some attempt have been made to analyze the deformation behavior of the sintered perform which helps to decide various parameters of the process in practical work and for industrial propose which are i) Equilibrium method ii) Upper bound method. The results obtained are discussed to illustrate the interaction of various parameters involved and are presented graphically.

Interfacial friction

Friction condition between deforming tool and work piece in metal working are of the greatest importance concerning a number of factors such as force and mode of deformation, properties of the finished specimen and resulting surface roughness. The relative velocity between the work piece material and the die surface together with high interfacial pressure and/or deformation modes will create the conditions essential for an adhesion in addition to sliding. For such a mechanism of composite friction, which usually occurs in plastic deformation of metal powder preforms, the shear equation becomes:

$$\tau = \mu \left[p + \rho_o \phi_o \right] \quad (1)$$

Where the first term on the right is the sliding friction and the second is the friction due to adhesion, which is due to change of the relative density of the preform. The change in relative density depends upon the deforming conditions such as speed and surface conditions.

During the compression of a metal powder preform the compressive force gradually increase the relative density, which latter is directly proportional to the real area of contact. The real area of contact grows and approaches the apparent area as the force increases which in turn increases the relative density.

The pattern of metal flow during the compression of a metal powder preform is such that there exists two zones, an inner one where no relative movement between work piece and die occurs (the sticking zone), and an outer zone where sliding occurs.

Therefore, the appropriate interfacial friction laws for different conditions given by Rooks [10] are:

$$\tau = \mu\left[P + \rho_o \phi_o \left\{1 - \left(\frac{r_m - r}{nb}\right)\right\}\right] \quad (2)$$

For the analysis of pressure distribution and die load, we will discuss Equilibrium method and upper bound method separately.

MATHEMATICAL MODELING

Case 1: Equilibrium method

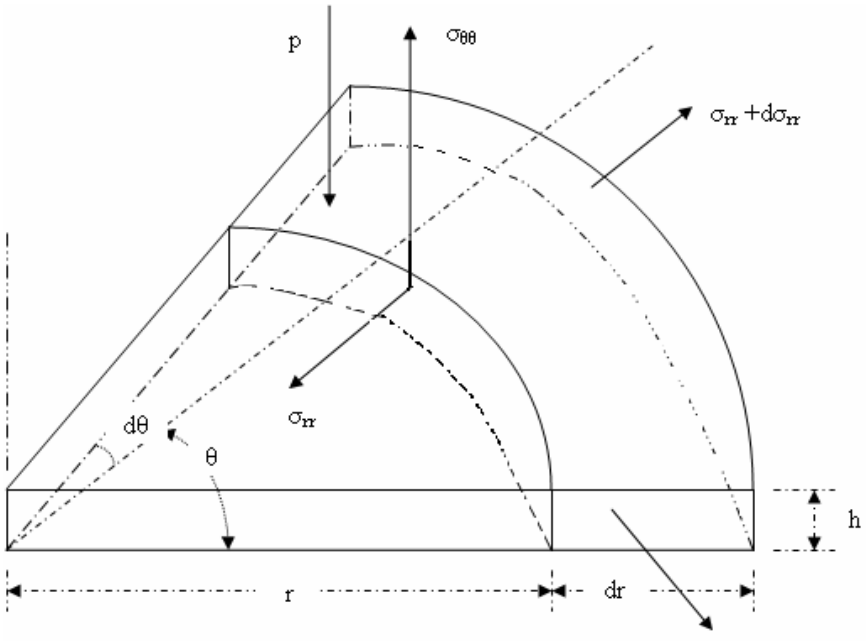

Figure-1. Force analysis of disc (Equilibrium method).

As we know that during the plastic deformation of the metal powder perform, the volume changes and the yielding of metal powder perform is not insensitive completely to the hydrostatic stress imposed. According to Tabata and Masaki [11]; the yield criterion is:

$$\rho^k \sigma_0 = \sqrt{3\, j_2}' + 3\eta\sigma_m \quad (3)$$

Or,

$$\rho^k \sigma_0 = \left[\{(\sigma_1 - \sigma_2)^2 + (\sigma_2 - \sigma_3)^2 + (\sigma_3 - \sigma_1)^2\}/2\right]^{1/2}$$

$$= \eta(\sigma_1 + \sigma_2 + \sigma_3)$$

As $\sigma_1 = \sigma_3 = \sigma_{rr}$ and $\sigma_2 = -p$ hence

$$(\sigma_1 - \sigma_2) \mp (2\sigma_1 + \sigma_2) = \rho^k \sigma_0$$

for the positive sign $\sigma_1 = \dfrac{\rho^k \sigma_0}{(2\eta+1)} - \dfrac{(\eta-1)}{(2\eta+1)}\sigma_2$ (4)

(a) Pressure distribution - considering the equilibrium of forces, which are acting on a volume element of the solid circular metal powder disc (Figure-1)

$$h\left[\sigma_{rr} r d\theta - \left(\sigma_{rr} + \frac{\partial \sigma_{rr}}{\partial r} dr\right)(r + dr)d\theta\right] + 2\tau r d\theta dr + 2\sigma_{\theta\theta} h dr \frac{d\theta}{2} = 0 \quad (5)$$

Ignoring all the increment of the order above 1 we get

$$-hr\frac{\partial \sigma_{rr}}{\partial r} - h(\sigma_{rr} - \sigma_{\theta\theta}) + 2\tau r = 0 \quad (6)$$

As $\sigma_{rr} = \sigma_{\theta\theta}$ so the above equation becomes

$$hd\sigma_{rr} - 2\tau dr = 0 \quad (7)$$

As from the equation (4)

$$\sigma_1 - \sigma_2 = \frac{\rho^k \sigma_0}{(2\eta+1)} - \frac{(\eta-1)}{(2\eta+1)}\sigma_2 - \sigma_2 = \lambda \text{ (say)}$$

As $\sigma_1 = \sigma_{rr}$ and $\sigma_2 = -p$ hence the equation becomes

$$\sigma_{rr} + p = \lambda$$

So, $d\sigma_{rr} + dp = 0$

With the help of this, equation (7) becomes

$$hdp + 2\tau dr = 0 \quad (8)$$

$$\tau = \mu\left[p + \rho_o \phi_o \left\{1 - \left(\frac{r_m - r}{nb}\right)\right\}\right]$$

As,

Assuming $\mu = \mu_1$ *and* $\mu = \mu_2$ for upper and bottom surface, therefore we get,

$$\frac{dp}{dr} + \frac{1}{h}(\mu_1 + \mu_2)\left[p + \rho_0\phi_0\left\{1 - \left(\frac{r_m - r}{nb}\right)\right\}\right] = 0$$

Or, $$\frac{dp}{dr} + \frac{(\mu_1 + \mu_2)}{h} p = \frac{-(\mu_1 + \mu_2)}{h}\rho_0\phi_0\left\{1 - \left(\frac{r_m - r}{nb}\right)\right\} \quad (9)$$

As this is first order linear differential equation of the type $\frac{dy}{dx} + Py = Q$ its solution is:

$$p = Ce^{\frac{-(\mu_1+\mu_2)}{h}} + \rho_0\phi_0\left\{\frac{r_m}{nb} - \frac{r}{nb} + \frac{h}{(\mu_1 + \mu_2)nb} - 1\right\} \quad (10)$$

as p = λ and r = b when $\sigma_{rr} = 0$

We get, $$C = e^{\frac{(\mu_1+\mu_2)b}{h}}\left[\lambda - \rho_0\phi_0\left\{\frac{r_m}{nb} - \frac{1}{n} + \frac{h}{(\mu_1 + \mu_2)nb} - 1\right\}\right] \quad (11)$$

Therefore,

$$p = e^{\frac{(\mu_1+\mu_2)(b-r)}{h}}\left[\lambda - \rho_0\phi_0\left\{\frac{r_m}{nb} - \frac{1}{n} + \frac{h}{(\mu_1 + \mu_2)nb} - 1\right\}\right] + \rho_0\phi_0\left\{\frac{r_m}{nb} - \frac{r}{nb} + \frac{h}{(\mu_1 + \mu_2)nb} - 1\right\}$$

$$\frac{p}{\lambda} = e^{\frac{(\mu_1+\mu_2)(b-r)}{h}}\left[1 - \frac{\rho_0\phi_0}{\lambda}\left\{\frac{r_m}{nb} - \frac{1}{n} + \frac{h}{(\mu_1 + \mu_2)nb} - 1\right\}\right] + \frac{\rho_0\phi_0}{\lambda}\left\{\frac{r_m}{nb} + \frac{h}{(\mu_1 + \mu_2)nb} - 1\right\} - \frac{\rho_0\phi_0}{\lambda}\frac{r}{nb} \quad (12)$$

Where $\rho_0\phi_0 = xp_{av}$; and x = 0.1, 0.2, 0.3, ……..

If $\mu_1 = \mu_2 = \mu$ then

$$\frac{p}{\lambda} = e^{\frac{2\mu(b-r)}{h}}\left[1 - \frac{\rho_0\phi_0}{\lambda}\left\{\frac{r_m}{nb} - \frac{1}{n} + \frac{h}{2\mu nb} - 1\right\}\right] + \frac{\rho_0\phi_0}{\lambda}\left\{\frac{r_m}{nb} + \frac{h}{2\mu nb} - 1\right\} - \frac{\rho_0\phi_0}{\lambda}\frac{r}{nb} \quad (13)$$

(b) Die load is given by

$$P = 2\pi\int_0^b prdr$$

By inserting the value of p in the above equation we get

$$P = 2\pi\left[A\left\{\frac{h^2}{(\mu_1 + \mu_2)^2} - e^{\frac{-(\mu_1+\mu_2)b}{h}}\frac{h}{(\mu_1 + \mu_2)}\left(b + \frac{h}{(\mu_1 + \mu_2)}\right)\right\} - B\frac{b^3}{3} + D\frac{b^2}{2}\right]$$

$$P = 2\pi A\frac{h^2}{(\mu_1 + \mu_2)^2} - 2\pi A\frac{h}{(\mu_1 + \mu_2)}\left\{b + \frac{h}{(\mu_1 + \mu_2)}\right\}e^{\frac{-(\mu_1+\mu_2)b}{h}} - \frac{2}{3}\pi Bb^3 + D\pi b^2 \quad (14)$$

If $\mu_1 = \mu_2 = \mu$ then

$$P = 2\pi\left[A\left\{\frac{h^2}{4\mu^2} - e^{\frac{-2\mu b}{h}}\frac{h}{2\mu}\left(b + \frac{h}{2\mu}\right)\right\} - B\frac{b^3}{3} + D\frac{b^2}{2}\right]$$

$$P = \frac{\pi A h^2}{2\mu^2} - \frac{Ah\pi}{\mu}\left(b + \frac{h}{2\mu}\right)e^{\frac{-2\mu b}{h}} - \frac{2\pi}{3}Bb^3 + D\pi b^2 \quad (15)$$

$$A = \lambda e^{\frac{(\mu_1+\mu_2)b}{h}}\left[1 - \frac{\rho_0\phi_0}{h}\left\{\frac{r_m}{nb} + \frac{h}{(\mu_1+\mu_2)nb} - \frac{1}{n} - 1\right\}\right];$$

$$B = \frac{\rho_0\phi_0}{nb};$$

$$D = \rho_0\phi_0\left(\frac{r_m}{nb} + \frac{h}{(\mu_1+\mu_2)nb} - 1\right)$$

If $\mu_1 = \mu_2 = \mu$ then

$$A = \lambda e^{\frac{2\mu b}{h}}\left[1 - \frac{\rho_0\phi_0}{h}\left\{\frac{r_m}{nb} + \frac{h}{2\mu nb} - \frac{1}{n} - 1\right\}\right]; B = \frac{\rho_0\phi_0}{nb};\ D = \rho_0\phi_0\left(\frac{r_m}{nb} + \frac{h}{2\mu nb} - 1\right)$$

Case 2: Upper bound method

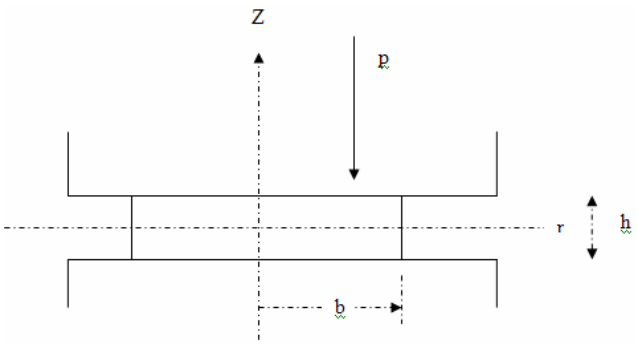

Figure-2. Schematic diagram of disc (Upper bound method).

(a) Velocity fields

$$U_r = \frac{(1-2\eta)Ur}{2(1+\eta)h};$$

$$U_z = -\frac{zU}{h};$$

$$U_\theta = 0; \quad (16)$$

(b) Strain rates

$$\dot{\varepsilon}_r = \frac{\partial \dot{U}_x}{\partial r} = \frac{(1-2\eta)U}{2(1+\eta)h}$$

$$\dot{\varepsilon}_\theta = \frac{U_r}{r} + \frac{\partial \dot{U}_\theta}{\partial \theta} = \frac{(1-2\eta)U}{2(1+\eta)h}$$

$$\dot{\varepsilon}_z = \frac{\partial \dot{U}z}{\partial z} = -\frac{U}{h} \quad (17)$$

The above normal-strain components satisfy the compressibility equation for porous materials [11]

$$\dot{\varepsilon}_r + \frac{(1-2\eta)}{2(1\pm\eta)}\dot{\varepsilon}_z = 0 \quad (18)$$

For plastic deformation of a metal powder the external power $\dot{J}^*$ supplied by the platens is given as-

$$\dot{J}^* = \dot{W}_i + \dot{W}_f + \dot{W}_a + \dot{W}_t \quad (19)$$

The first term on the right hand side i.e W_i denotes the rate of internal energy dissipation, the second term W_f denotes the frictional shear energy losses, the third term W_a denotes the energy dissipation due to inertia forces, and the last term W_t covers power supplied by predetermined body tractions. In this case forces due to inertia are negligibly small and no external surface traction is stipulated. Therefore, $W_a = W_t = 0$.

Now the external power $\dot{J}^*$ supplied by the press through the platen is -

$$\dot{J}^* = \int F_i U_i ds = PU \quad (20)$$

(c) Internal power of deformation

The plastic work done per unit volume is given by:

$$dW_i = \frac{\sqrt{2}}{3}\rho^k\lambda\sqrt{\left(\dot{\varepsilon}_r - \dot{\varepsilon}_\theta\right)^2 + \left(\dot{\varepsilon}_\theta - \dot{\varepsilon}_z\right)^2 + \left(\dot{\varepsilon}_z - \dot{\varepsilon}_r\right)^2} \quad (21)$$

So, $W_i = \frac{\rho^k \lambda U}{(1+\eta)} \pi b^2$ (22)

(d) Energy dissipation due to friction

$$W_f = \int_v \tau \left| \Delta v \right| ds \quad (23)$$

Considering magnitude of relative velocity,

$$\left| \Delta v \right| = \frac{(1-2\eta)Ur}{2(1+\eta)h}$$

$ds = rd\theta dr$

$$\tau = (\mu_1 + \mu_2)\left[p + \rho_0 \phi_0 \left\{ 1 - \left(\frac{r_m - r}{n r_0} \right) \right\} \right]$$

Where $\rho_0 \phi_0 = x.p_{av}$ and $p = \frac{P}{\pi b^2}$

x = 0.1, 0.2, 0.3, ……..

Put all the values in equation (23), and after integration we can get,

$$W_f = \frac{1}{3} \frac{\pi(\mu_1 + \mu_2)(1-2\eta)Ub^3}{(1+\eta)h} \left[p + \rho_0 \phi_0 \left\{ 1 + \frac{3}{4nb} - \frac{r_m}{nb} \right\} \right] \quad (24)$$

If $\mu_1 = \mu_2 = \mu$ then

$$W_f = \frac{2}{3} \frac{\pi\mu(1-2\eta)Ub^3}{(1+\eta)h} \left[p + \rho_0 \phi_0 \left\{ 1 + \frac{3}{4nb} - \frac{r_m}{nb} \right\} \right] \quad (25)$$

(e) Die load

$$J^* = W_i + W_f = \text{PU}$$

$$P = \frac{\rho^k \lambda \pi b^2}{(1+\eta)} + \frac{1}{3} \frac{\pi(\mu_1 + \mu_2)(1-2\eta)b^3}{(1+\eta)h} \left[p + \rho_0 \phi_0 \left\{ 1 + \frac{3}{4nb} - \frac{r_m}{nb} \right\} \right] \quad (26)$$

If $\mu_1 = \mu_2 = \mu$ then

$$P = \frac{\rho^k \lambda \pi b^2}{(1+\eta)} + \frac{2}{3} \frac{\pi\mu(1-2\eta)b^3}{(1+\eta)h} \left[p + \rho_0 \phi_0 \left\{ 1 + \frac{3}{4nb} - \frac{r_m}{nb} \right\} \right] \quad (27)$$

Now, $p = \frac{P}{\pi b^2}$; for $\rho_0 \phi_o = x.p = x\frac{P}{\pi b^2}$

$$P = \left[1 - \frac{1}{3} \frac{b(\mu_1 + \mu_2)(1-2\eta)}{(1+\eta)h} - \frac{1}{3} \frac{b(\mu_1 + \mu_2)(1-2\eta)x}{(1+\eta)h} \left\{ 1 + \frac{3}{4nb} - \frac{r_m}{nb} \right\} \right]^{-1} \left[\frac{\rho^k \lambda \pi b^2}{(1+\eta)} \right] \quad (28)$$

$$\frac{P}{\lambda} = \left[1 - \frac{1}{3} \frac{b(\mu_1 + \mu_2)(1-2\eta)}{(1+\eta)h} - \frac{1}{3} \frac{b(\mu_1 + \mu_2)(1-2\eta)x}{(1+\eta)h} \left\{ 1 + \frac{3}{4nb} - \frac{r_m}{nb} \right\} \right]^{-1} \left[\frac{\rho^k \pi b^2}{(1+\eta)} \right] \quad (29)$$

$\mu_1 = \mu_2 = \mu$ then

$$P = \left[1 - \frac{2}{3} \frac{b\mu(1-2\eta)}{(1+\eta)h} - \frac{2}{3} \frac{b\mu(1-2\eta)x}{(1+\eta)h} \left\{ 1 + \frac{3}{4nb} - \frac{r_m}{nb} \right\} \right]^{-1} \left[\frac{\rho^k \lambda \pi b^2}{(1+\eta)} \right] \quad (30)$$

$$\frac{P}{\lambda} = \left[1 - \frac{2}{3} \frac{b\mu(1-2\eta)}{(1+\eta)h} - \frac{2}{3} \frac{b\mu(1-2\eta)x}{(1+\eta)h} \left\{ 1 + \frac{3}{4nb} - \frac{r_m}{nb} \right\} \right]^{-1} \left[\frac{\rho^k \pi b^2}{(1+\eta)} \right] \quad (31)$$

EXPERIMENTAL PROCEDURE

1. Metal powder used

(a) Aluminium powder

Atomized aluminium powder of purity 99.5% and finer than 100 μm was used throughout the experiments. The powder was supplied by M/s Mahindra Sintered Products Limited, Pune, India. The physical and chemical

property of aluminium powder is given in Tables 1 and 2, respectively.

Table-1. Physical characteristics of atomized aluminium powder used.

Screen analysis (micron)	+100	-100 +150	-150 +200	-200 +240	-240 +350	-350
Percentage weight retained	0	36.00	15.00	14.00	21.00	14.50

Apparent density 1.20 g/cc
Tap density 2.54 g/cc

Table-2. Chemical Analysis of Sintered aluminium Powder (Weight Percentage).

Maximum Limits of Impurities:

Iron contents	0.17%
Copper	0.00159%
Silicon	0.1313%
Manganese	0.0023%
Magnesium	0.00160%
Zinc	0.0053%
Hydrogen loss	0.4879%

(b) Copper powder

Electrolytic Copper powder of greater than 99% purity was used for preparation of test piece. The powder was supplied by M/s Mahindra Sintered Products Limited, Pune, India. The physical and chemical property of Copper powder is given in Tables 3 and 4, respectively.

Table-3. Physical characteristics of copper powder used.

Screen analysis (micron)	+100	-100 +150	-150 +200	-200 +240	-240 +350	-350
Percentage weight retained	0	35.00	15.00	14.50	20.00	14.50

Apparent density 2.60 g/cc
Tap density 8.96 g/cc

Table-4. Chemical analysis of sintered copper powder (weight percentage).

Copper	99.80%
Phosphorous	< 0.001%
Iron	< 0.006%
Silicon	< 0.002%

2. Preparation of specimens and density measurement

In the preparation of metal powder compacts the following steps are necessary:

I. Compaction
II. Sintering
III. Machining

(I) Compaction

Metal powder was compacted in a closed circular die (bore ϕ 30 mm) using a 150 Ton hydraulic press at various recorded pressures. The die wall was lubricated with fine graphite powder. Few green cylindrical aluminium and copper powder compacts of about 30 mm diameter were obtained by this process. The compaction arrangement is shown in Figure-3.

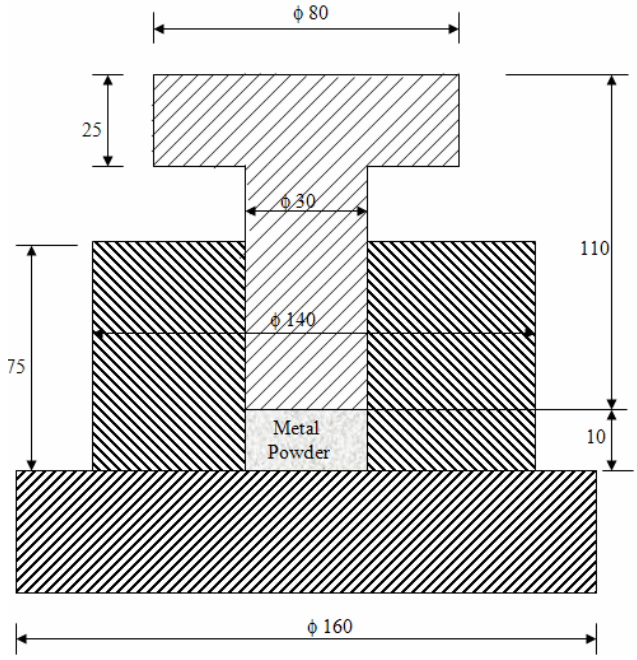

Figure-3. Arrangement for compaction of metal powder preform (circular type).

(II) Sintering

The basic purpose of sintering is to develop mechanical strength in the metal powder compacts. Sintering of aluminium and copper compacts was carried out at 450 and 850^{0}C, respectively for two hours in an endothermic sand atmosphere. All sintering operations were carried out in a muffle type silicon carbide furnace capable of providing sintering temperature unto 1300^{0}C with an accuracy of ± 5^{0}C. In order to minimize the non-uniformity of density distribution, the sintered compacts were re-pressed at the same compaction pressure in the same die. The specimens were resintered at the same temperature and time.

(III) Machining

The specimens were made by machining the compacts to the desired dimensions. The surfaces of the specimens were polished with fine emery paper.

Density of the metal powder preforms was obtained simply by measuring specimen dimensions and weight. In order to confirm this density the hydrostatic (or Archimedes) method was also employed. The relative density of the powder preform was obtained by the ratio of the powder preform density to the solid metal density.

3. Experimental procedure and measurements

Experiments were conducted on a Universal Testing Machine using appropriate dies. The metal powder preform of known relative density was placed inside the conical converging dies and was compressed at room temperature by applying the load. The compression was carried out in dry and lubricated conditions. Fine graphite powder was applied as lubricant. The following important measurements were made:

(i) Increase in the relative density of the preform with increase in compressive load.
(ii) Variation of p/λ (Relative forging pressure) of the perform with the percentage reduction in height.
(iii) Variation of p/λ (Relative forging pressure) of the perform with change in density at 40% reduction in height of the metal powder perform.
(iv) Increase in the relative density of the preform with increase in p/λ (Relative forging pressure).

The experimental procedure was repeated for five compacts under the similar processing conditions and an average reading was recorded.

RESULTS AND DISCUSSIONS

In metal powder forming operation, there are two processes that happen simultaneously i.e., compaction (densification) and deformation. Initially compaction dominates; so relative average pressure curve increases slowly. After compaction phase deformation dominates and a steep slope is observed. Material flows mainly in the direction of punch movement, with little lateral flow in the starting. As the density increases, lateral flow increases. In the final stage of deformation, the lateral flow approach the spreading behavior of pore free material. Lateral/spreading increases with increasing initial density of preform.

For parametric analysis of deformation behavior of sinter metal perform during open die forging, let us assume following set of data for various processing parameters.

$n = 1, 2$

$\mu_1 = 0.3$, $\mu_2 = 0.3, 0.35, 0.4, 0.45$

$x = 0.1, 0.2$

$\rho = 0.70, 0.75, 0.80, 0.85, 0.90, 0.95$

Percentage reduction in height of the perform = 10%, 20%, 30%, 40%.

Figure-4. Deformed Cu metal powder performs after 43% reduction in height.

Figure-5. Al compact.

Figure-6. Cu compact.

Figure-7. Sintering furnace.

Figure-8. Hydraulic press.

Figure-9 shows the variation of relative average forging pressure (p/λ) with relative density of sintered preform by both equilibrium and Upper bound method.

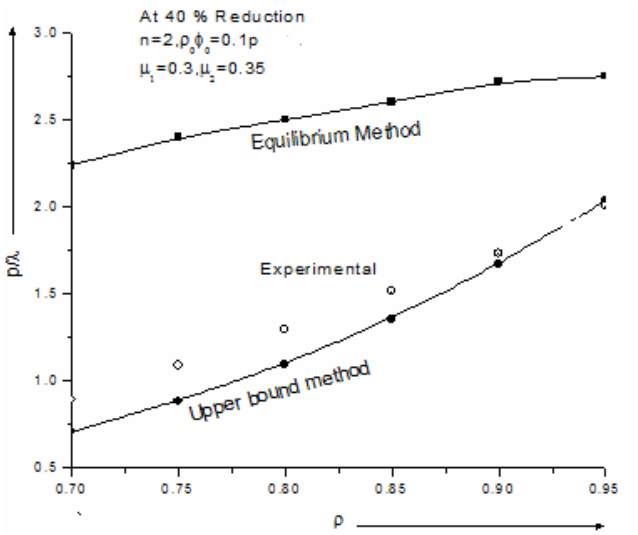

Figure-9. Theoretical and experimental variation of relative compressive pressure with density.

The curves express the theoretical results at 40% reduction of the circular preform for different values of the coefficient of friction at upper and bottom surfaces. As relative density of the sintered perform increases, the required amount of relative forging pressure increases. It is seen that the experimental values of the relative forging pressure is nearly in close agreement with the theoretical values obtained from equation (29) by upper bound method. Figures 10 and 11 shows the variation in relative average forging pressure (p/λ) with percentage reduction in height of the metal powder perform at different initial relative density by equilibrium method and Upper bound method, respectively at n = 2 with different values of the coefficient of friction at upper and bottom surface, that mean μ_1 (upper surface) = 0.3, μ_2 (bottom surface) = 0.35.

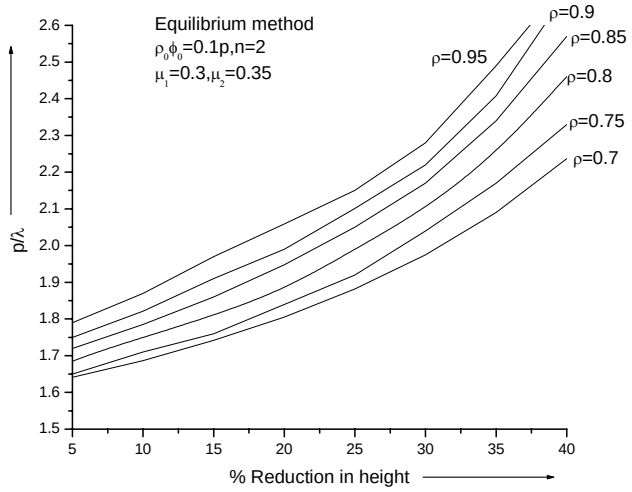

Figure-10. Theoretical variation of relative compressive pressure with % reduction in height of the sintered metal powder perform by Equilibrium method at different initial relative density.

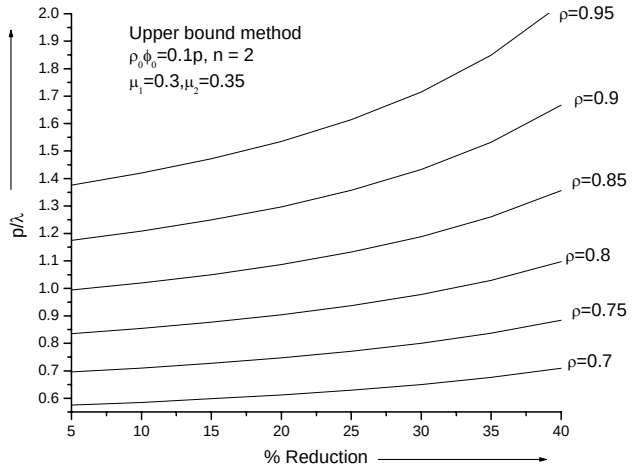

Figure-11. Theoretical variation of relative compressive pressure with % reduction in height of the sintered metal powder perform by Upper bound method at different initial relative density.

These figures show the variation of relative density with average relative forging pressure. Initially large amount of relative average forging pressure is consumed in densification of the perform. After attaining sufficient densification, deformation occurs significantly. That's why initially a nearly flat curve is observed for all the metal powder performs having different initial relative densities.

Figures 12 to 14 shows variation in p/λ (Relative forging pressure) with % reduction in height of the metal powder perform by both the methods at ρ = 0.8 μ_1 = 0.3and at different values of μ_2 .We take $\rho_0\phi_0$ = 0.1 p.

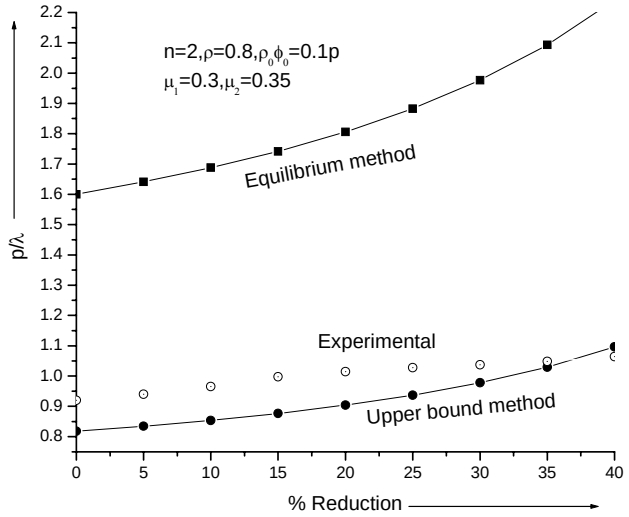

Figure-12. Theoretical variation of relative compressive pressure with % reduction in height of the sintered metal powder perform by Equilibrium and upper bound method at different friction values of the upper and bottom surface.

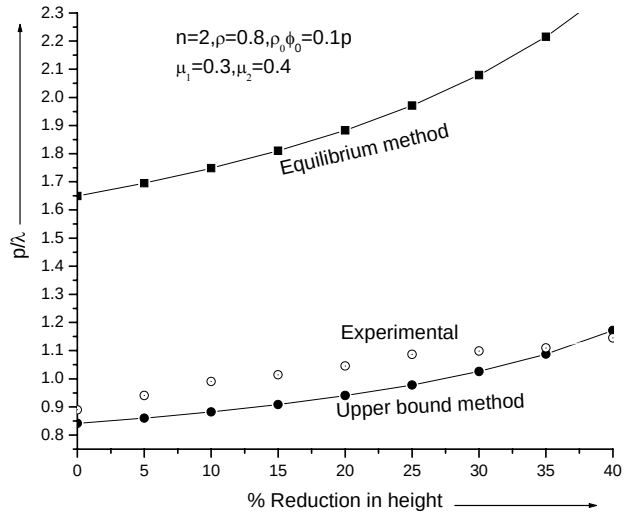

Figure-13. Theoretical variation of relative compressive pressure with % reduction in height of the sintered metal powder perform by Equilibrium and upper bound method at different friction values of the upper and bottom surface.

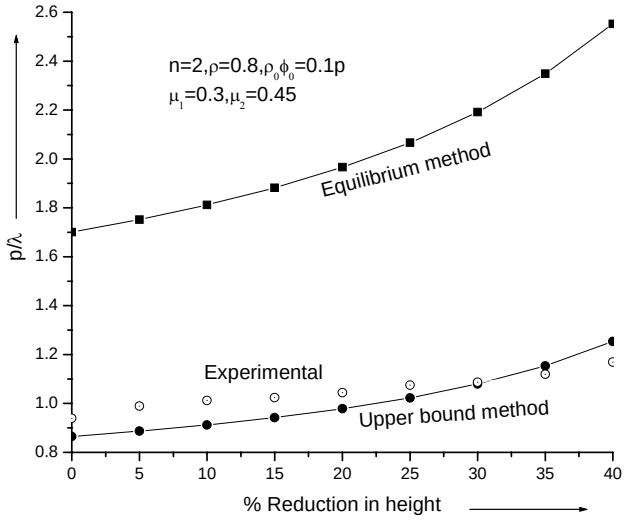

Figure-14. Figure-14 Theoretical variation of relative compressive pressure with % reduction in height of the sintered metal powder perform by Equilibrium and upper bound method at different friction values of the upper and bottom surface.

Figures 15 and 16 shows variation in p/λ (Relative forging pressure) with % reduction in height of the metal powder perform by both the methods at ρ = 0.8 μ_1 = 0.3 and at different values of μ_2. We take different values of $\rho_0\phi_0$.

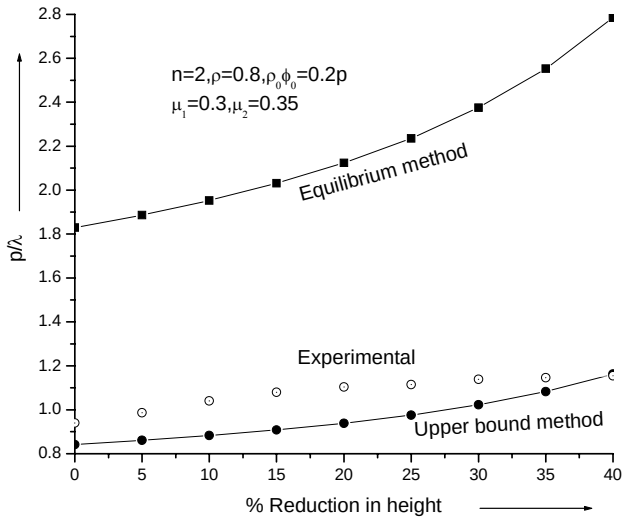

Figure-15. Theoretical variation of relative compressive pressure with % reduction in height of the sintered metal powder perform by Equilibrium and upper bound method at different friction values of the upper and bottom surface.

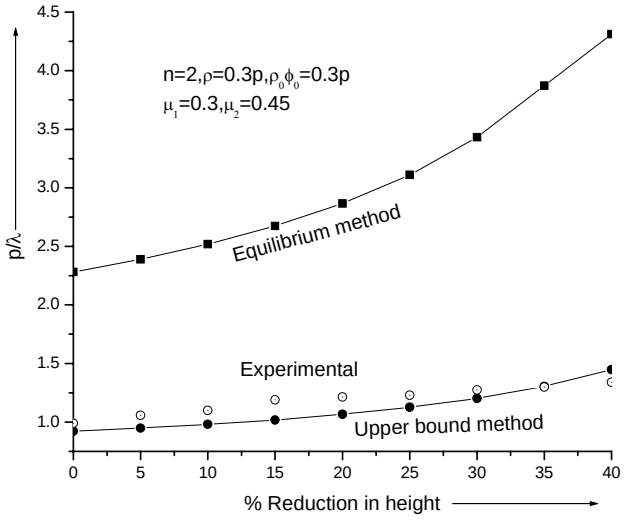

Figure-16. Theoretical variation of relative compressive pressure with % reduction in height of the sintered metal powder perform by Equilibrium and upper bound method at different friction values of the upper and bottom surface.

These figures shows the theoretical compressive relative pressure versus percentage reduction. The curves express the theoretical results for a particular initial relative density of the square preform and for various values of the coefficient of friction at upper and bottom surfaces. The compressive relative pressure is found to increase with increase in percentage reduction in height and the coefficient of friction, compressive relative pressure is also found to increase with increase in the value of $\rho_0\phi_0$.

Figure-17 shows the variation of relative forging pressure with percentage reduction in height at n = 1.

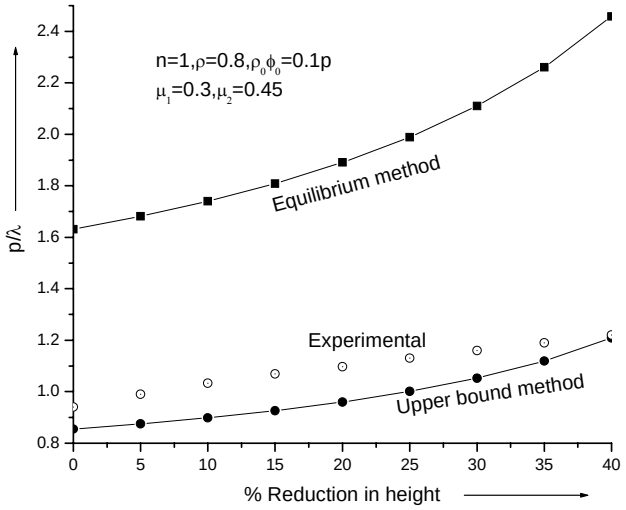

Figure-17. Theoretical variation of relative compressive pressure with % reduction in height of the sintered metal powder perform by Equilibrium and upper bound method at different friction values of the upper and bottom surface.

Figures 18 and 19 show that variation of forging load with percentage reduction in the height of the preform in the case of Cu and Al by both the methods at ρ = 0.8, $\rho_0\phi_0$ = 0.1p, μ_1 = 0.3 and μ_2 = 0.45 , n = 2.

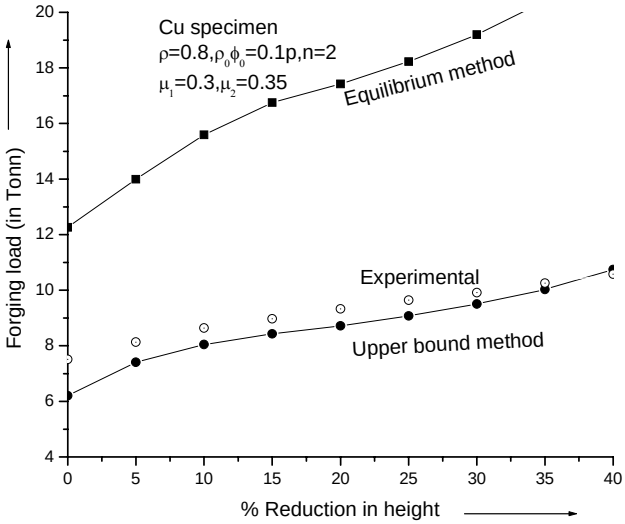

Figure-18. Theoretical variation of relative compressive load with % reduction in height of the sintered metal powder perform of Cu by Equilibrium and upper bound method at different friction values of the upper and bottom surface.

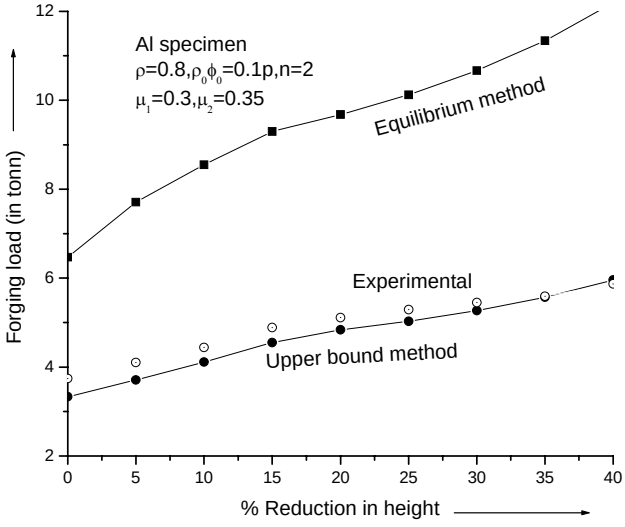

Figure-19. Theoretical variation of relative compressive load with % reduction in height of the sintered metal powder perform of Al by Equilibrium and upper bound method at different friction values of the upper and bottom surface.

It also feels that as initial relative density of the sintered perform increases, the relative average forging pressure increases. Also a higher value of relative average forging pressure has been observed theoretically during mathematical analysis by Equilibrium method. It is due to the fact in equilibrium method we do not consider any

loses due to flow a condition i.e., Velocity fields are not mentioned and pressure distribution is ignored due to velocity field. Equilibrium method considers forces at every point are in equilibrium but force distribution is not mentioned but upper bound method considers the losses due to velocity discontinuity. Force, Stress and pressure distribution are taken into account in upper bound method.

CONCLUSIONS

During forging of powder preforms, the mode of deformation is quite different from wrought materials and it is function of both density and hydrostatic stress. In powder forging, mass constancy is to be assumed. During forging of metal powder preforms it is seen that compaction and compression both take place simultaneously. Initially the closing of pores dominates the compression process. The larger amount of applied load is utilized in densification and lesser amount is consumed for compression.

A composite interfacial friction law has been taken for studying the deformation characteristics of the sintered porous materials. The relative average forging pressure increases with increasing percentage reduction of height of the perform and coefficient of friction. The work will found to be effective for the determination of die loads during the forging of porous metal bars by using Upper Bound approach as compare to the equilibrium method approach.

REFERENCES

[1] P.F. Thomson. 1986. Densification of sintered metal compacts by cold deformation. J. Mech. Working Tech. 13(2): 219- 227.

[2] 2001. Cost savings win the day for PM parts. Metal Powder Report. 56(7- 8): 10 -12.

[3] A. K. Jha, S. Kumar. 1994. Production of sinter-forged components. J. Mater Process. Tech. 41: 143-169.

[4] S. Singh, A.K. Jha. 2001. Sintered preforms add better value to aerospace components. J. Aerospace Engg. I. E. (1) 82: 1-6.

[5] E. Ilia, K. Tutton, M.O' Neill. 2005. Forging a way towards a better mix of PM automotive steels. Metal Powder Report. 60(3): 38-44.

[6] A.K. Jha, S. Kumar. 1996. Forging of metal powder performs. Int. J. Mach. Tool Design Res. 23(210).

[7] L. M. M. Alvesa, P.A.F. Martinsa, J.M.C. Rodrigues. 2006. A new yield functions for porous materials. J. Mater. Process. Tech. 179(1-3): 36-43.

[8] A.K. Jha, S. Kumar. 1978. Deformation characteristics and fracturing of sintered copper powder strips during cold forging. J. Mech. Work Technol. 16 (1988) 145. Sci. Technol. 22(2): 45.

[9] S. Malayappan, G. Esakkimuthu. 2006. Barreling of aluminium solid cylinders during cold upsetting with differential frictional conditions at the faces. Int. J. Adv. Manuf. Tech. 29: 41-48.

[10] B. W. Rooks. 1974. The effect of die temperature on metal flow and die wear during high speed hot forging. 15th Int. MTDR conference held in Birmingham, 18-20 September. p. 487.

[11] T Tabata, S Masaki and K Hosokawa. 1980. Int. J. Powder Metal, Powder Technol. 16: 149.

Nomenclature

2b = Diameter of the perform
r = Radius of the perform
h = Instantaneous thickness of perform
r_m =Sticking Zone radius
μ_1 = Coefficient of friction of upper surface
μ_2 = Coefficient of friction of lower surface
ρ = Relative density of the perform
P = Die load
σ_0 = Yield stress of the non-work hardening matrix metal
$\dot{\varepsilon}_r, \dot{\varepsilon}_\theta, \dot{\varepsilon}_z$ = Principal strain increment
η = Constant and a function of ρ only
J_2' = Second invariant of deviatoric stress
r, θ, z = Cylindrical co-ordinates
p = ram pressure
P = Die load
ρ_0 = A dimensional ratio ($=\rho_r/\rho_*$)
ϕ_0 = specific cohesion of a contact surface
τ = Shear stress
k = Constant equal to 2 in yield criterion
n = A constant quantity
λ = Flow stress of metal powder perform
ρ_*, ρ_r = Densities of apparent and real contact areas